

# Expansion of the Hadley cell under global warming

Jian Lu<sup>1</sup> Gabriel A. Vecchi<sup>2</sup> Thomas Reichler<sup>3</sup>

<sup>1</sup>Advanced Study Program/NCAR

<sup>2</sup>Geophysical Fluid Dynamical Laboratory/NOAA

<sup>3</sup>Department of Meteorology, University of Utah

## 1. Introduction

The Hadley Cell (HC) plays a pivotal role in the earth's climate by transporting energy and angular momentum poleward and by organizing the three dimensional tropical atmospheric circulation. Here, we investigate the response of the structure and intensity of the HC to green house gas (GHG) induced global warming by examining the A2 scenario simulations from the Fourth Assessment Report (AR4) of the Intergovernmental Panel on Climate Change (IPCC). We find that there is a robust poleward expansion and weakening of the HC across most the AR4 models. Associated with this widening is a poleward expansion of the subtropical dry zone, which is demarcated by the isopleths of  $P=E$  in the subtropics. We also try to identify the possible mechanisms for the expansion of the HC based on simple scaling theories.

## 2. Results

- ❑ The hydrological response to global warming is, overall a reinforcement of the global climatological background pattern (Figure 1).
- ❑ Poleward expansion of the subtropical dry zone. The edges of the dry zone displace poleward by  $\sim 1^\circ$  in each hemisphere for the multi-model ensemble mean of the A2 scenario (Figure 1a).
- ❑ The poleward expansion of the subtropical dry zone is strongly tied to the poleward expansion of the HC (Figure 2).
- ❑ The magnitude of the expansion is a function of the GHG forcing (Figure 2).
- ❑ 85% (72%) of the scatter in the poleward displacement of the subtropics dry zones in the southern (northern) hemisphere can be explained by a linear relation to the displacements of the outer boundaries of the HC (Figure 2).
- ❑ The ensemble mean intensity of the Hadley Cell weakens for both the annual mean (by  $\sim 2.5\%$ ) and seasonal mean circulation (by  $\sim 6.5\%$ ) (Figure 3).
- ❑ Poleward expansion of the Hadley cell in both hemisphere, especially the winter cell (Figure 3).
- ❑ The poleward mass transport at the upper branch of the HC takes place more aloft than usual (Figure 3).

## 3. Possible mechanisms for HC expansion

Two alternative views on the controls of the HC have guided much of the understanding of the width of the HC. On one hand, nearly inviscid theory for axisymmetric circulation (no eddies) (Held and Hou, 1980) predicts that the meridional extent of the HC scales as

$$\phi_H \sim \left( \frac{gH_t}{\Omega^2 a^2} \frac{\Delta_h}{\theta_0} \right)^{\frac{1}{2}}, \quad (1)$$

where  $H_t$  is the height of the tropical tropopause (TTH),  $\theta_0$  is global mean temperature,  $\Delta_h$  is the equator-to-pole surface potential temperature difference in radiative equilibrium, and other parameters have their conventional meanings. This scaling relation, which suggests no dependence on static stability, is derived by assuming that (i) the zonal wind in the upper branch of the HC is angular-momentum conserving and (ii) the HC is energetically closed, so that the diabatic heating in the ascent regions is balanced by the diabatic cooling in the descent regions. The second view sees the width of the HC as being determined by the poleward extent to which the angular-momentum conservation continues until the resulting vertical shear becomes baroclinically unstable (Held, 2000). Solving the equation between the angular momentum conserving zonal wind and the baroclinically critical zonal wind yields an alternative scaling for the width of the HC:

$$\phi_H \propto \left( \frac{NH_e}{\Omega a} \right)^{\frac{1}{2}}, \quad (2)$$

wherein the two-layer model's criterion (Phillips, 1954) for instability has been used.  $H_e$  is the local tropopause height,  $N$  the vertically averaged Brunt-Väisälä frequency, indicative of the tropospheric gross static stability. If the scaling relation (1) applies to the HC expansion under GHG forcing, variations of the HC width should be proportional to the tropical tropopause height. On the other hand, if the scaling (2) applies, one may expect the extent of the Hadley circulation to be sensitive to the gross stability and the tropopause height near the poleward boundary of the circulation.

First, we plot for each model the change in TTH during the 21<sup>st</sup> century against that of the HC extent, the former being estimated as the negative of the pressure anomalies at the tropopause and averaged within 20° to the equator, and the latter defined as the distance between the southern and northern edges of the HC. Both quantities were normalized by the increase of the global mean temperature seen in the individual models during the 21st century. Comparing different models, the individual long-term trends in HC extent show no correlation to the trends in TTH (Figure 4a). In fact, within each model, the detrended annual mean time series of TTH and HC extent tend to be anti-correlated, in stark contrast to the positive correlations of the time series with trend (Figure 4b). This hints that distinct mechanisms govern the long-term widening of the HC under global warming and its interannual variability.

The extratropical tropopause height (ETH, averaged over 35°-55°), is found to be closely related to the variation of the HC extent not only within each model (Figure 4d), but also in the comparison of the long-term trend among models (Figure 4c). A similar relationship has been found between the HC extent and the gross stability. Indeed, the ETH is very strongly correlated with the local gross stability (with correlations of ~0.95) within most models examined and hence can be thought of as a good proxy of the ETH. The change in mid-latitude tropopause height (or stability) not only explains over 60% of the variance in the spread of the HC widening across the AR4 models, but also accounts

for the consensus HC expansion at a rate of  $1.2^\circ$  per 10hPa rise in the ETH in the A2 scenario. The relevance of the ETH to the HC extent in the natural climate variability can also be readily discerned from their correlations of the detrended time series in Figure 4d.

From this analysis, one is tempted to argue that scaling relation (2) is a better model for the extent of the HC. The HC extent in the present-day climate may be interpreted as being limited by the latitude at which the thermally driven wind becomes baroclinically unstable, rather than by the energetic closure of the thermally driven cell.

#### 4. Conclusions

In response to increased GHG forcing, we find a robust weakening and poleward expansion of the Hadley circulation in simulations of the 21<sup>st</sup> century climate taken from the A2 scenario of the IPCC AR4 project. In accord with the movement of the HC, the subtropical dry zones also expand poleward. Further analysis suggests that the consensus of the HC expansion in the AR4 models is unlikely to originate from tropical processes, despite the fact that tropical heating is effective in driving the variation of the HC at interannual time scales, and that it accounts for significant part of the inter-model variability in HC expansion. We find that extratropical tropopause height, which is a good proxy of the gross static stability, varies in concert with the width of the HC on both the interannual and longer time scales. Under global warming conditions, rising tropospheric static stability, which is an established consequence of moist thermodynamics, stabilizes the subtropical jet streams at the poleward flank of the Hadley Cell to baroclinic instability, as a result the edges of the HC expand poleward.

#### Acknowledgement

We thank Kirk Bryan, Isaac Held, Dargan Frierson, and Qian Song for their perceptive comments and useful discussions during the formative stage of this paper. We acknowledge the international modeling group for providing their data for analysis, the Program for Climate Model Diagnosis and Intercomparison (PCMDI) for collecting and archiving the model data, the JSC/CLIVAR Working Group on Coupled Modeling (WGCM) and their Coupled Model Intercomparison Project (CMIP) and Climate Simulation Panel for organizing the model data and analysis activity, and the IPCC WG1 TSU for technical support. The IPCC Data Archive at Lawrence Livermore National Laboratory is supported by the Office of Science, U. S. Department of Energy. J. Lu is supported by the Visiting Scientist Program of the University Corporation for Atmospheric Research (UCAR).

#### References

- [1] Held, I. M., 2000, The general circulation of the atmosphere. *Proc. Program in Geophysical Fluid Dynamics*. Woods Hole Oceanographic Institution, Wood Hole, MA. <http://gfd.whoi.edu/proceedings/2000/PDFvol2000.html>
- [2] Held, I. M. and A. Y. Hou, 1980, Nonlinear axially symmetric circulations in a nearly inviscid atmosphere, *J. Atmos. Res.*, **37**, 515-533
- [3] Phillips, N. A., 1954, Energy transformations and meridional circulations associated with simple baroclinic waves in a two-level, quasi-geostrophic model, *Tellus VI*, **3**, 273-286

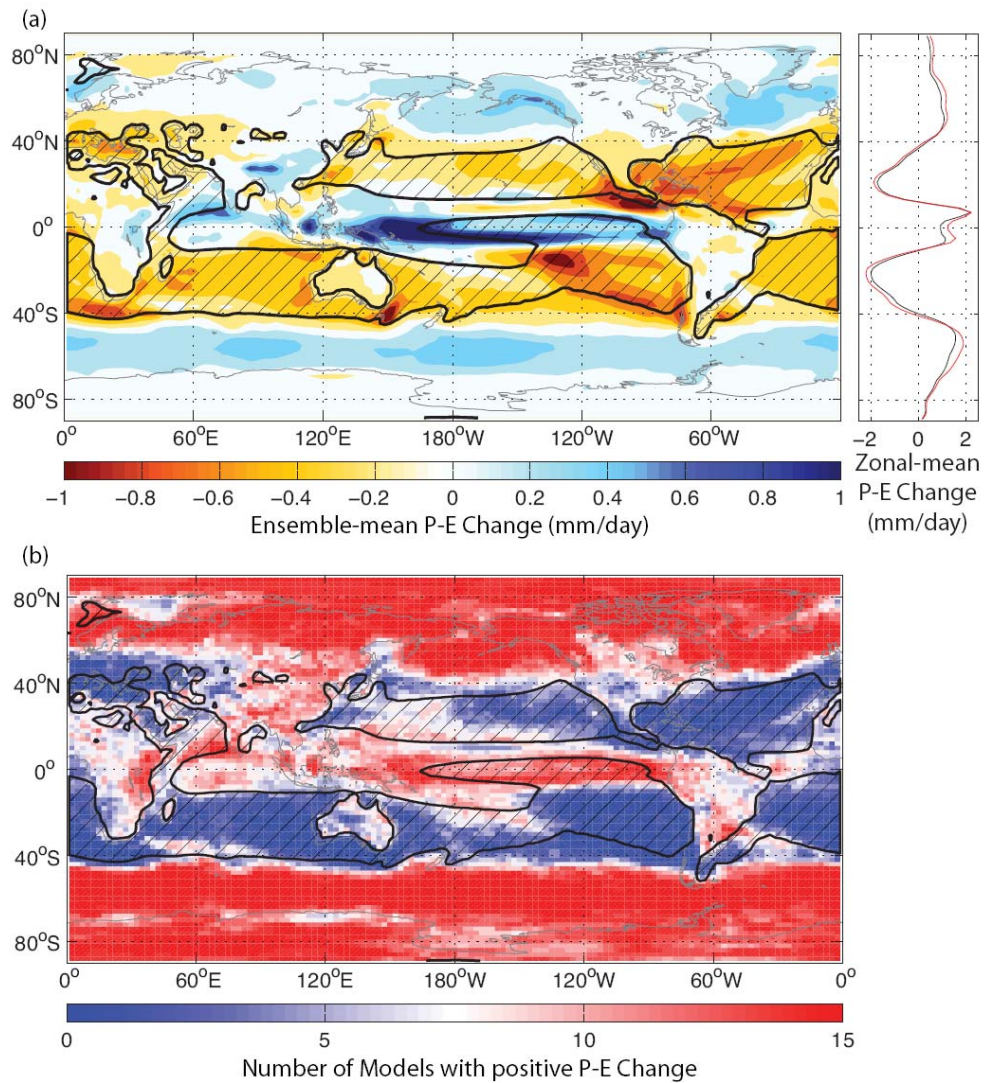


**Figure 1** (a) The multi-model ensemble mean  $P-E$  in the A2 scenario. Shading indicates the difference between the first and the last 20 years of the 21<sup>st</sup> century and the black line denotes the 0-isopleths averaged from 2001 to 2020. The right sub-panel shows the zonal mean averaged over 2001-2020 (black) and 2081-2100 (red). Units are mm/day. (b) Number count out of the total 15 models that simulate a moistening (i.e.,  $\Delta(P - E) > 0$ ) at each grid point.

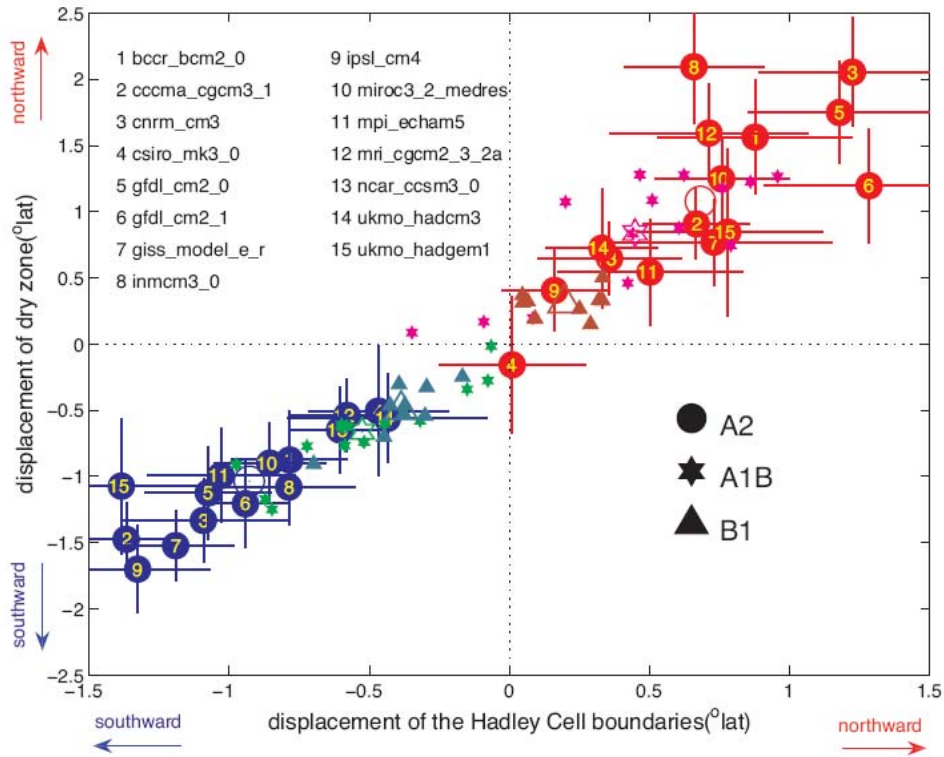


**Figure 2** The breakdown by models and scenarios of the displacement of the northern (warm colors) and southern (cold colors) edges of the subtropical dry zone (y-axis) versus that of the HC (x-axis). The circles, hexagrams, and triangles denote the changes (2081-2100 minus 2001-2020) estimated from the A2, A1B and B1 scenarios, respectively. The open symbols denote the multi-model ensemble mean values. The cross on each circle shows the 95% confidence interval of the estimated displacements using Student's t-test.

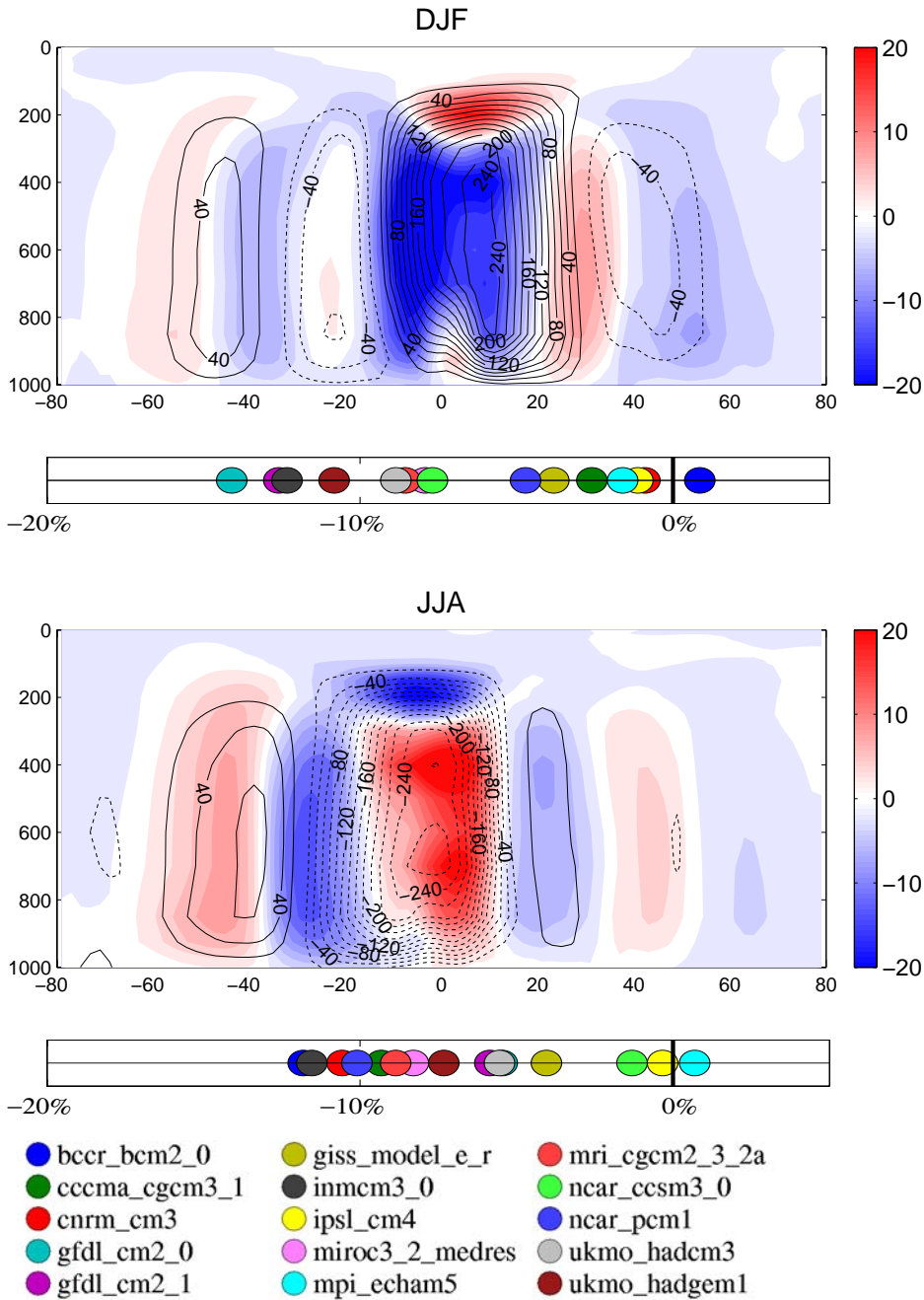


**Figure 3** The zonal-mean mass flux streamfunction for the annual mean DJF (upper) and JJA (lower) seasons. The shading indicates the multi-model ensemble mean differences between 2081-2100 and 2001-2020 from A2 scenario, the contours the climatological streamfunction based on years 2001-2020. The color coded dots indicate the fractional change in the intensity of the HC for each of the 15 models. The intensity of the HC is defined as the maximum (minimum) of the winter cell for DJF (JJA) season.

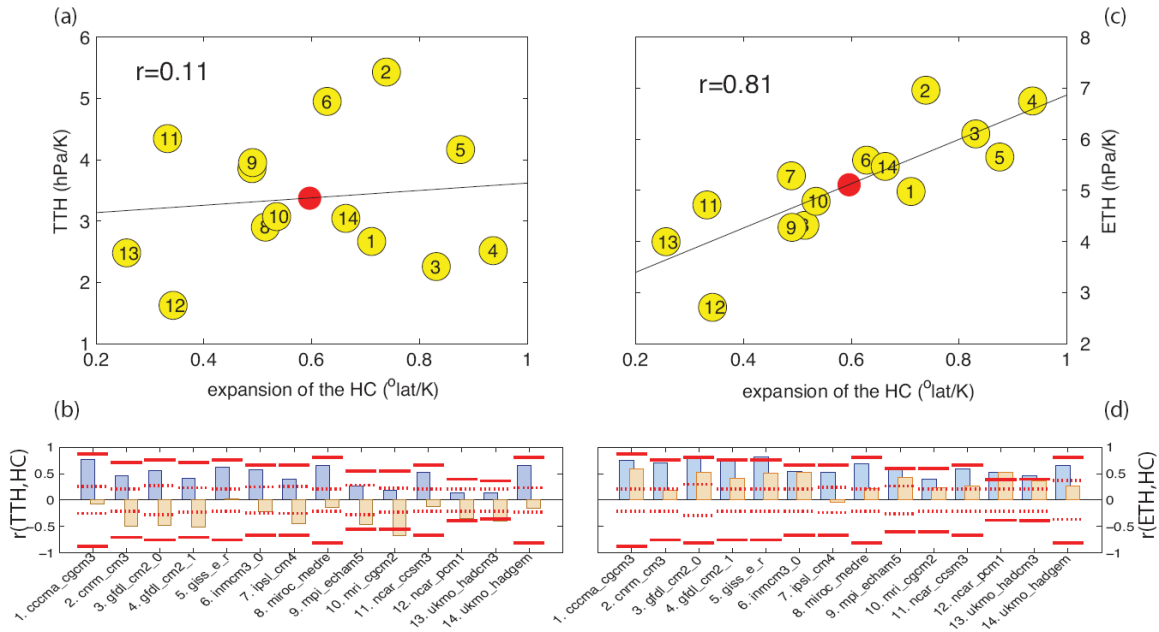


**Figure 4** The relationship of the tropical (20°S-20°N) tropopause height (TTH, left panels); the extra-tropical (35°S-55°S and 35°N-55°N) tropopause height (ETH, right panels) with the extent of the HC for 14 models from the A2 scenario. Positive tropopause height value represents rise of tropopause. Upper panels show the differences between (2081-2020) and (2001-2020), normalized by the corresponding change in the global mean temperature. The red dots denote the multi-model ensemble mean values. Lower panels show the correlation coefficients between the full (blue bars) and detrended (sandy bars) time series of the HC extent and TTH (b) and ETH (d). The horizontal lines indicate the P=0.05 confidence level of the correlation for each model based on Student's t-test. During the computation of the confidence levels, the reduction of effective degrees of freedom due to the autocorrelations of the time series has been considered. The solid (dotted) lines are estimated from the full time series containing trend (detrended time series).